

Oriented Crystallization of Calcium Carbonate under Self-Organized Monolayers of Amide-Containing Phospholipids

Peter J. J. A. Buijnsters,^{†,‡} Jack J. J. M. Donners,[#] Susan J. Hill,[§]
Brigid R. Heywood,[§] Roeland J. M. Nolte,^{†,#} Binne Zwanenburg,[‡] and
Nico A. J. M. Sommerdijk^{*,#}

Department of Organic Chemistry, NSR-Center, University of Nijmegen, Toernooiveld 1,
NL-6525 ED Nijmegen, The Netherlands, Laboratory of Macromolecular and
Organic Chemistry, Eindhoven University of Technology, Eindhoven, The Netherlands,
Birchall Centre for Inorganic Chemistry and Materials Science, Keele University,
Keele, United Kingdom

Received December 18, 2000. In Final Form: March 7, 2001

In the presence of calcium ions amide-containing phospholipid **1** self-assembles to form well-defined two-dimensional domains at the air–water interface. These domains act as templates for the crystallization of calcium carbonate that efficiently nucleate the growth of [10.0] oriented calcite irrespective of the surface concentration of the lipid. Responsible for this preference for nucleation at the (10.0) face is the formation of an intramolecular hydrogen bond between the phosphate group and the phenoxy moiety which forces the phosphate group to adopt a bidentate orientation toward the aqueous phase. It was shown that when this hydrogen bond was absent, that is, when the phosphate group is monomethylated, lateral pressure was required in order to enforce a similar conformation and accomplish the nucleation of [10.0] oriented calcite.

Introduction

Crystal formation in Nature is often mediated and regulated by highly organized organic surfaces of biopolymers.¹ The processes involving crystallization are very well controlled, and the resulting crystals possess shapes and sizes that are distinctly different from those obtained under abiotic conditions.² The relationship between the templating biomolecular substrate and the inorganic phase lies in the epitaxial matching of lattice spacings of specific crystal planes with some ordered arrangement of molecular units in the template.³ To mimic and to understand biological mineralization, researchers have carried out different types of experiments. One approach has been to isolate the templating matrix from mineralized tissues and examine the growth of calcium salts in the presence of this matrix.⁴ Other experiments have focused on synthetic (bio-)organic templates, such as polymers,⁵ macromolecular complexes,⁶ phospholipid

vesicles,⁷ β -pleated poly(amino acids) entrapped in gelatin,⁸ self-assembled monolayers on gold substrates,⁹ and Langmuir films.^{10,11} In the case of Langmuir monolayers the amphiphilic molecules can be designed in such a way that they act as artificial two-dimensional nuclei for the promotion of crystal nucleation. Such films have been used as templates to direct the crystal nucleation and growth of amino acids,¹¹ ice,¹² proteins,¹³ and calcium carbonate.¹¹

Initially, monolayer crystallization experiments were conducted on highly compressed surfactant films which acted as 2D crystals requiring the monolayer to match exactly one of the crystal faces of the nucleating species.^{10,11} It was found that modification of the apolar part of the surfactant¹⁴ as well as the headgroup¹⁵ had a marked effect

* Corresponding author. E-mail: N.Sommerdijk@tue.nl.

[†] Present address: Department of Medicinal Chemistry, Janssen Research Foundation, Beerse, Belgium.

[‡] University of Nijmegen.

[#] Eindhoven University of Technology.

[§] Keele University.

(1) Weiner, S. *Crit. Rev. Biochem.* **1986**, *20*, 365. (b) Mann, S.; Archibald, D. D.; Didymus, J. M.; Douglas, T.; Heywood, B. R.; Meldrum, F. C.; Reeves, N. J. *Science* **1993**, *261*, 1286.

(2) Addadi, L.; Weiner, S. *Angew. Chem.* **1992**, *104*, 159.

(3) Mann, S. *Nature* **1988**, *332*, 119.

(4) Addadi, L.; Weiner, S. *Proc. Natl. Acad. Sci. U.S.A.* **1985**, *82*, 4110. (b) Addadi, L.; Weiner, S. *Mol. Cryst. Liq. Cryst.* **1986**, *134*, 305. (c) Albeck, S.; Weiner, S.; Addadi, L. *Chem. Eur. J.* **1996**, *2*, 278. (d) Levi, Y.; Albeck, S.; Brack, A.; Weiner, S.; Addadi, L. *Chem. Eur. J.* **1998**, *4*, 389. (e) Kniep, R.; Busch, S. *Angew. Chem., Int. Ed. Engl.* **1996**, *35*, 2624.

(5) Berman, A.; Ahn, D. J.; Lio, A.; Salmeron, M.; Reichert, A.; Charych, D. *Science* **1995**, *269*, 515. (b) Calvert, P.; Rieke, P. *Chem. Mater.* **1996**, *8*, 1715. (c) Reis, R. L.; Cunha, A. M.; Fernandes, M. H.; Correia, R. N. *J. Mater. Sci. Mater. Med.* **1997**, *8*, 897. (d) Epple, M.; Schwarz, K. *Chem. Eur. J.* **1998**, *4*, 1898. (e) Cölfen, H.; Antonietti, M. *Langmuir* **1998**, *14*, 582.

(6) Donners, J. J. J. M.; Heywood, B. R.; Meijer, E. W.; Nolte, R. J. M.; Roman, C.; Schenning, A. P. H. J.; Sommerdijk, N. A. J. M. *Chem. Commun.* **2000**, 1937.

(7) Mann, S.; Hannington, J. P.; Williams, R. J. P. *Nature* **1986**, *324*, 565. (b) Ozin, G. A. *Acc. Chem. Res.* **1997**, *30*, 17.

(8) Falini, G.; Fermani, S.; Gazzano, M.; Ripamonti, A. *Chem. Eur. J.* **1997**, *3*, 1807. (b) Falini, G.; Fermani, S.; Gazzano, M.; Ripamonti, A. *Chem. Eur. J.* **1998**, *4*, 1048.

(9) Archibald, D. D.; Quadri, S. B.; Gaber, B. P. *Langmuir* **1996**, *12*, 538. (b) Wurm, D. B.; Brittain, S. T.; Kim, Y.-T. *J. Mater. Sci. Lett.* **1996**, *15*, 1285. (c) Küther, J.; Nelles, G.; Seshadri, R.; Schaub, M.; Butt, H.-J.; Tremel, W. *Chem. Eur. J.* **1998**, *4*, 1834. (d) Küther, J.; Seshadri, R.; Tremel, W. *Angew. Chem., Int. Ed. Engl.* **1998**, *37*, 3044. Aizenberg, J.; Black, A. J.; Whitesides, G. M. *J. Am. Chem. Soc.* **1999**, *121*, 4500.

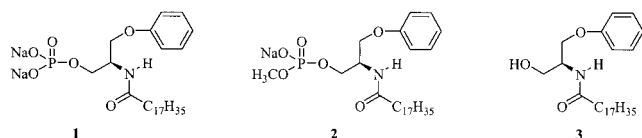
(10) Landau, E. M.; Levanon, M.; Leiserowitz, L.; Lahav, M.; Sagiv, J. *Nature* **1985**, *318*, 353. (b) Landau, E. M.; Popovitz-Biro, R.; Levanon, M.; Leiserowitz, L.; Lahav, M.; Sagiv, J. *Mol. Cryst. Liq. Cryst.* **1986**, *134*, 323.

(11) Mann, S.; Heywood, B. R.; Rajam, S.; Birchall, J. D. *Nature* **1988**, *324*, 692. (b) Landau, E. M.; Grayer Wolf, S.; Levanon, M.; Leiserowitz, L.; Lahav, M.; Sagiv, J. *J. Am. Chem. Soc.* **1989**, *111*, 1436. (c) Rajam, S.; Heywood, B. R.; Walker, J. B. A.; Mann, S.; Davey, R. J.; Birchall, J. D. *J. Chem. Soc., Faraday Trans.* **1991**, *87*, 727. (d) Heywood, B. R.; Mann, S. *Chem. Mater.* **1994**, *6*, 311.

(12) Popovitz-Biro, R.; Wang, J. L.; Majewski, J.; Shavit, E.; Leiserowitz, L.; Lahav, M. *J. Am. Chem. Soc.* **1994**, *116*, 1179.

(13) Ahlers, M.; Muller, W.; Reichert, A.; Ringsdorf, H.; Venzmer, J. *Angew. Chem., Int. Ed. Engl.* **1990**, *29*, 1269.

Chart 1



on the crystallization processes. Also, the mobility of the molecules in the monolayer turned out to have significant influence, viz. on the homogeneity and nucleation density of the crystallization as well as on the morphology of the overgrowth. Later hydrogen bonding functionalities, such as amide bonds, were introduced in the surfactants which could interlink the amphiphilic molecules into larger arrays, overcoming the necessity to compress the molecules into the desired organization in which they exert their nucleation effect.¹⁶

In previous work we reported on the aggregation behavior of amide-containing phospholipid surfactants which form highly organized, chiral aggregates in water and at the air-water interface.¹⁷ The expression of chirality on the supramolecular level could be achieved by fine-tuning the interactions between the molecules, for example by pH variation or metal ion complexation. In this work we already demonstrated that the aggregate morphology of the amide-containing phospholipid **1** (Chart 1) can be altered through compensation of headgroup charge. It was expected, therefore, that addition of calcium ions could be used to further structure the highly organized assemblies of phospholipid **1**. It was anticipated that such assemblies of these self-organized amphiphilic molecules could serve as well-defined templates directing the crystallization of inorganic compounds, in particular CaCO_3 .

Experimental Section

Synthesis. Thin-layer chromatography analyses were performed on Merck precoated silica gel 60 F254 plates (0.25 mm) using the solvent mixtures indicated, and spots were visualized with UV and/or using ammonium molybdate (25 g/L) and ceric ammonium sulfate (10 g/L) in 10% aq H_2SO_4 . Phosphate-containing compounds were visualized using Knight and Young¹⁸ spray. Flash column chromatography was performed on Merck kieselgel 60H (0.005–0.040 mm) using a pressure of ~0.5 bar using the eluents indicated. Melting points were measured on a Reichert thermopan microscope. Optical rotations were determined at 20 °C using a Perkin-Elmer automatic polarimeter, model 241. Routine FT-IR spectra were recorded using a Biorad WIN-IR FTS-25 single-beam spectrometer. ^1H , ^{13}C , and ^{31}P NMR spectra were recorded on a Bruker AC 300 (300/75.1/121 MHz) spectrometer. Chemical shifts are reported in ppm (δ) relative to Me_4Si or trimethyl phosphate as internal standard. Mass spectra were recorded with a double-focusing VG 7070E spectrometer. Elemental analyses were performed with a Carlo Erba Instruments EA 1108 element analyzer.

Disodium (-)-(2*S*)-3-Phenoxy-2-octadecanoylamino-propan-1-yl Phosphate (1). This compound was synthesized according to the procedure of Sommerdijk et al.¹⁹ Mp 145–147 °C. $R_f = 0.30$ (MeOH/ H_2O / CHCl_3 , 39/10/67, v/v/v). $t_R = 14.20$ min (capillary electrophoresis). $[\alpha]_D^{20} = 22.1$ ($c = 1.0$, $\text{CHCl}_3/\text{MeOH}$,

9/1 (v/v)). ^{31}P NMR (CDCl_3): $\delta = -0.751$ ppm. IR (KBr): $\nu = 3300$ (N–H) cm^{-1} , 3090 (C–H, aryl), 2915, 2840 (C–H, alkyl), 1630 (Am I), 1600 (C=C, aryl), 1545 (Am II), 1240 (P=O). MS [FAB⁺, m/z] = 580 [$M + \text{Na}^+$], 557 [M^+]. Anal. Calcd for $\text{C}_{27}\text{H}_{46}\text{NO}_6\text{PNa}_2 \cdot 3.5\text{H}_2\text{O}$: C, 51.50; H, 8.64; N, 2.22. Found: C, 51.18; H, 8.12; N, 2.33.

Benzyl (-)-(2*S*)-3-Phenoxy-2-octadecylaminopropan-1-yl Methyl Phosphate. Anhydrous sodium iodide (132 mg, 0.880 mmol) was added to a stirred solution of dibenzyl (2*S*)-3-phenoxy-2-octadecanoylamino-propan-1-yl phosphate (534 mg, 0.770 mmol) in dry acetone (6 mL) and heated under reflux for 3 h and subsequently left to stand for 48 h at –20 °C, after which a white precipitate was obtained.²⁰ This precipitate was washed with cold acetone (5 × 5 mL), dried under reduced pressure, dissolved in dry acetone (75 mL), treated with ion-exchange resin (3 g, Dowex 50WX20, H⁺-form), and finally heated under reflux for 5 h. The ion-exchange resin was removed by filtration, and the filtrate was concentrated in vacuo. The residue was treated with diazomethane in diethyl ether (10 mL, 0.3 M), stirred overnight, and concentrated in vacuo, after which the remaining material was purified by flash column chromatography (Si_2O , hexane/ethyl acetate, 3:1 (v/v)) to give 143 mg (30%) of the product as a colorless oil. $R_f = 0.30$ (Si_2O , hexane/ethyl acetate, 3:1 (v/v)). $[\alpha]_D^{20} \approx 0$ ($c = 1.0$, CHCl_3). ^1H NMR (CDCl_3 , 300 MHz): $\delta = 7.36$ – 6.88 (m, 10H, OC_6H_5 , $\text{OCH}_2\text{C}_6\text{H}_5$), 6.34 (m, 1H, NH), 5.07–5.03 (m, 2H, $\text{OCH}_2\text{C}_6\text{H}_5$), 4.50–4.48 (m, 1H, C(O)NHCH), 4.30–3.93 (m, 4H, $\text{CH}_2\text{OC}_6\text{H}_5$, $\text{CH}_2\text{OP}(\text{O})(\text{OCH}_3)$), 3.71–3.66 (m, 3H, $\text{OP}(\text{O})(\text{OCH}_3)$), 2.15 (t, $J = 6.9$ Hz, 2H, $\text{C}_{16}\text{H}_{33}\text{CH}_2\text{C}(\text{O})$), 1.61 (m, 2H, $\text{C}_{15}\text{H}_{31}\text{CH}_2\text{CH}_2\text{C}(\text{O})$), 1.26 (m, 28H, $\text{CH}_3(\text{CH}_2)_{14}$, $\text{C}_2\text{H}_4\text{C}(\text{O})$), 0.94 (t, $J = 7.6$ Hz, 3H, $\text{CH}_3\text{CH}_2\text{C}(\text{O})$). ^{13}C NMR (CDCl_3 , 75 MHz): $\delta = 173.90$ (C(O)NH), 158.81 (quart $\text{CH}_2\text{OC}_6\text{H}_5$), 136.22, 136.14 (quart P(O)CH₂(OC_6H_5)), 130.20 (P(O)CH₂($m\text{-OC}_6\text{H}_5$)), 129.40 (P(O)CH₂($o\text{-OC}_6\text{H}_5$)), 129.31 ($m\text{-CH}_2\text{OC}_6\text{H}_5$), 128.65 (P(O)CH₂($p\text{-OC}_6\text{H}_5$)), 121.95 ($p\text{-CH}_2\text{OC}_6\text{H}_5$), 115.17 ($o\text{-CH}_2\text{OC}_6\text{H}_5$), 70.35, 70.27 (P(O)CH₂(OC_6H_5)), 66.72, 66.64 ($\text{CH}_2\text{OP}(\text{O})\text{CH}_2$), 65.78 ($\text{CH}_2\text{OC}_6\text{H}_5$), 55.18, 55.10 ((O)P(O)CH₃), 37.27 ($\text{CH}_2\text{C}(\text{O})\text{NH}$), 32.57–23.33 ($\text{CH}_3(\text{CH}_2)_{15}\text{CH}_2\text{C}(\text{O})$), 14.76 ($\text{CH}_3(\text{CH}_2)_{15}\text{CH}_2\text{C}(\text{O})$). ^{31}P NMR (CDCl_3 , 121 MHz) $\delta = -2.14$, –2.20 ppm.²¹ MS [FAB⁺ m/z] = 640 [$M + \text{Na}^+$], 618 [$M + 1^+$].

Sodium (-)-(2*S*)-3-Phenoxy-2-octadecylaminopropan-1-yl Methyl Phosphate (2). Benzyl (2*S*)-3-phenoxy-2-octadecylaminopropan-1-yl methyl phosphate (142 mg, 0.230 mmol), dissolved in methanol (50 mL), was subjected to hydrolysis for 1 h with Pd(C) as the catalyst. The catalyst was removed using a small RP-18 column washed with hot methanol (5 × 25 mL), and the filtrate was concentrated in vacuo to a volume of approximately 25 mL before 10 mL of water containing NaOH (4.5 mg, 0.113 mmol) was added. This solution was treated with Dowex 50WX20 (Na⁺-form) and lyophilized to afford 126 mg (100%) of **2** as a white hygroscopic, fluffy powder. $R_f = 0.50$ ($\text{CHCl}_3/\text{MeOH}/\text{H}_2\text{O}$, 67/39/10). $t_R = 12.91$ min (capillary electrophoresis). $[\alpha]_D^{20} = -8.3$ ($c = 1.0$, CHCl_3). ^{31}P NMR (CDCl_3 , 121 MHz) $\delta = -0.4881$. IR (KBr, cm^{-1}): ν 3600–3200 (H_2O), 3030 (C–H aromatic), 2918, 2850 (C–H alkyl), 1643 (Am I), 1543 (Am II), 1467 (C–H deformation, alkyl), 1246 (P=O). MS ((FAB⁺); m/z): 1121 [$M_2 + \text{Na} + 1^+$], 572 [$M + \text{Na}^+$], 550 [$M + 1^+$]. Anal. Calcd for $\text{C}_{28}\text{H}_{49}\text{NO}_6\text{PNa} \cdot 4\text{H}_2\text{O}$: C, 52.70; H, 8.30; N, 2.19. Found: C, 52.40; H, 8.10; N, 2.14.

(-)-(2*R*)-3-Phenoxy-2-octadecanoylamino-propan-1-ol (3). Sodium iodide (10 mg, 0.067 mmol) was added to a stirred solution of (-)-(2*S*)-1-octadecanoyl-2-phenoxy-methylaziridine¹⁹ (172.8 mg, 0.417 mmol) in dry acetonitrile (25 mL). The reaction mixture was heated under reflux for 2 h, and the resulting mixture was concentrated in vacuo. Dichloromethane (25 mL) was added to the residue, and the solution was washed with water (3 × 10

(14) Landau, E. M.; Wolf, S. G.; Levanon, M.; Leiserowitz, L.; Lahav, M.; Sagiv, J. *J. Am. Chem. Soc.* **1989**, *111*, 1436.

(15) Mann, S.; Heywood, B. R.; Rajam, S.; Walker, J. B. A. *J. Phys. Appl. Phys.* **1991**, *24*, 154. (b) Heywood, B. R.; Mann, S. *Chem. Mater.* **1994**, *6*, 311.

(16) Cooper, S. J.; Sessions, R. B.; Lubetkin, S. D. *J. Am. Chem. Soc.* **1998**, *120*, 2090. (b) Champ, S.; Dickinson, J. A.; Fallon, P. S.; Heywood, B. R.; Mascall, M. *Angew. Chem., Int. Ed. Engl.* **2000**, *39*, 2716.

(17) Sommerdijk, N. A. J. M.; Buijnsters, P. J. J. A.; Akdemir, H.; Geurts, Pistorius, A. M. A.; Feiters, M. C.; Nolte, R. J. M.; Zwanenburg, B. *Chem. Eur. J.* **1998**, *4*, 127.

(18) Knight, R. H.; Young, L. *Biochem. J.* **1958**, *70*, 111.

(19) See Sommerdijk, N. A. J. M.; Buijnsters, P. J. J. A.; Akdemir, H.; Geurts, D. G.; Nolte, R. J. M.; Zwanenburg, B. *J. Org. Chem.* **1997**, *62*, 4955.

(20) See also: Zervas, L.; Dilaris, I. *J. Am. Chem. Soc.* **1955**, *77*, 5354.

(21) During the course of the reaction sequence an additional stereogenic center is formed on the phosphorous atom which results in the formation of two diastereomers which are observed as two separate peaks in the ^{31}P NMR spectrum. See also: (a) Stegerhoek, L. J.; Verkade, P. E. *Recl. Trav. Chim. Pays-Bas* **1958**, *77*, 133. (b) Gielkens, J. W.; Hoefnagel, M. A.; Stegerhoek, L. J.; Verkade, P. E. *Recl. Trav. Chim. Pays-Bas* **1958**, *77*, 656.

mL). The separated organic layer was dried (Na_2SO_4), and the solvent was removed in vacuo. The residue (169.1 mg) was dissolved in ethanol (15 mL), and to this solution was added oxalic acid (60 mg, 0.67 mmol). The reaction mixture was heated under reflux for 3 h and then concentrated in vacuo. The residue was purified by flash column chromatography (Si_2O , hexane/ethyl acetate, 1:1 (v/v)) to furnish 119 mg (66%) of **3**. $R_f = 0.25$ (Si_2O , hexane/ethyl acetate, 1:1). Mp 87.2–89.0 °C. $[\alpha]_D^{20} -3.6$ ($c = 1.0$, CHCl_3). $^1\text{H NMR}$ (CDCl_3 , 300 MHz): $\delta = 7.36\text{--}6.89$ (m, 5H, OC_6H_5), 6.14 (m, 1H, C(O)NHCH), 4.32–4.27 (m, 1H, C(O)NHCH), 4.18–4.07 (ABX, $J_{\text{AX}} = 4.11$ Hz, $J_{\text{BX}} = 4.78$ Hz, $J_{\text{AB}} = 9.52$ Hz, 2H, $\text{CH}_2\text{OC}_6\text{H}_5$), 3.97–3.76 (ABX, $J_{\text{AX}} = 4.65$ Hz, $J_{\text{BX}} = 4.64$ Hz, $J_{\text{AB}} = 11.2$ Hz, 2H, CH_2OH), 2.23 (t, $J = 7.4$ Hz, 2H, $\text{C}_{16}\text{H}_{33}\text{CCH}_2\text{C(O)}$), 1.64 (m, 2H, $\text{C}_{15}\text{H}_{31}\text{CCH}_2\text{CH}_2\text{C(O)}$), 1.25 (m, 28H, $\text{CH}_3(\text{CH}_2)_{14}\text{C}_2\text{H}_4\text{C(O)}$), 0.88 (t, $J = 6.8$ Hz, 3H, $\text{CH}_3(\text{CH}_2)_{16}$). $^{13}\text{C NMR}$ (CDCl_3 , 75 MHz): $\delta = 174.49$ (C(O)NH), 159.23 (quat OC_6H_5), 130.23 ($m\text{-OC}_6\text{H}_5$), 122.01 ($o\text{-OC}_6\text{H}_5$), 115.13 ($p\text{-OC}_6\text{H}_5$), 67.89 ($\text{CH}_2\text{OC}_6\text{H}_5$), 63.54 (CH_2OH), 51.07 (CHNH), 37.44–23.36 ($(\text{CH}_2)_{16}\text{CH}_3$), 14.80 ($\text{CH}_3(\text{CH}_2)_{16}$). IR (KBr, cm^{-1}): ν 3668 (O–H), 3307 (N–H), 3100–3050 (C–H aromatic), 2950–2850 (C–H alky), 1641 (Am I), 1549 (Am II). MS [EI m/z , rel int (%)] = 433 ($[\text{M}^+]$, 0.5), 415 ($[\text{C}_{27}\text{H}_{45}\text{NO}_2^+]$, 2.6), 340 ($[\text{C}_{21}\text{H}_{42}\text{NO}_2^+]$, 100), 284 ($[\text{C}_{18}\text{H}_{38}\text{NO}^+]$, 14.5), 94 ($[\text{C}_5\text{H}_6\text{O}^+]$, 19.9). Anal. Calcd for $\text{C}_{27}\text{H}_{47}\text{NO}_3 \cdot 0.25\text{H}_2\text{O}$: C, 74.01; H, 10.93; N, 3.20. Found: C, 74.01; H, 11.05; N, 3.16.

Capillary Electrophoresis. The purity of compounds **1** and **2** was also checked with capillary electrophoresis (CE). The system consisted of a Hewlett-Packard CE apparatus operated at 30 kV and 20 °C. A buffer ($\text{Na}_2\text{B}_4\text{O}_7/\text{NaOH}$, 50 mM, pH = 9.3) containing 26.7 mM β -cyclodextrine (to prevent aggregate formation) was used, and the effluent was monitored at 197 nm. Samples were dissolved in the buffer and injected by applying 5 mbar of pressure (10 s).

Aggregation Experiments. A 2% (w/v) aqueous solution (50 μL) of phospholipids **1** or **2** was injected in water or an aqueous solution containing 9 mM CaCl_2 to a final concentration of 0.1% (w/v, phospholipid/water), sonicated for 15 min at 60 °C, and then left to stand for 24 h at room temperature before electron microscopy samples were prepared. Samples were prepared by placing a drop of the dispersion onto a carbon-coated Formvar-covered copper transmission electron microscope grid. The excess of the dispersion was removed after 1 min by blotting with filter paper, and subsequently the sample was dried and negatively stained with an aqueous 1% (w/v) ammonium molybdate or 1% (w/v) uranyl acetate solution. After 30 s the excess of the staining solution was removed by blotting with a filter paper and the specimen was dried for at least 4 h at room temperature.

Monolayer Experiments. All glassware was cleaned prior to use with a HF solution (10% in water (v/v)), washed several times with ultrapure water (Labconco Water Pro System, resistance 18 M Ω), rinsed with ethanol (p.a. quality), and dried under a N_2 -flow. Monolayer experiments were performed with a thermostated double-barrier R&K trough (6 cm \times 25 cm) using a compression speed of 4.4 cm^2/min . The surface pressure of the monolayers was measured using a Wilhelmy plate which was calibrated with octadecanol. The surface of the compressed monolayers was studied with a Brewster angle microscope (NFT BAM-1) mounted on a home-built trough with dimensions 14.0 cm \times 21.0 cm. The surface pressure was measured using Wilhelmy plates which were calibrated with octadecanol and were mounted on a Trans-Tek transducer (Connecticut, USA). The rate of compression was 4.4 cm^2/min . The surfactant was spread using a chloroform solution (**1** and **2**) or a chloroform/methanol (9/1 (v/v)) solution (**3**) (10 μL , 1 mg/mL). Compression was started after 10 min.

Crystallization Experiments. Supersaturated solutions of calcium bicarbonate were prepared using the method of Kitano.²² Carbon dioxide gas was bubbled through a stirred aqueous (Labconco Water Pro System, resistance 18 M Ω) suspension of CaCO_3 (6.3 g/2.5 L) at a rate of $\sim 0.2 \text{ m}^3 \cdot \text{h}^{-1}$ for a period of 1.5 h. The suspension was then filtered and the filtrate purged with

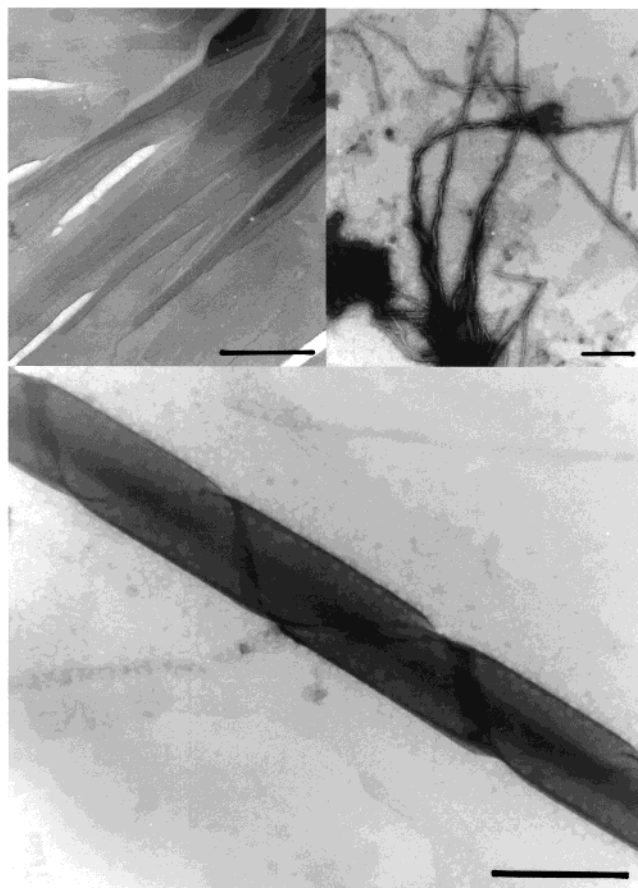


Figure 1. Electron micrographs taken from 0.1% (w/v) dispersions of (a) **1** (Pt shadow technique, bar 250 nm), (b) **1** after addition of 10 mM CaCl_2 (negative staining, bar 500 nm), and (c) **2** after addition of 10 mM CaCl_2 (negative staining, bar 500 nm).

carbon dioxide gas for 0.5 h to dissolve any remaining crystals. All crystallization experiments were performed in rigorously cleaned glass crystallization dishes. Compressed films were formed by adding known amounts of surfactant to generate a liquid- or solidlike film at the air–water interface. Crystals were harvested after 20 h on cover slips dipped through the films and were mounted on scanning electron microscope (SEM) specimen stubs. A JEOL T330 SEM operating at 15 keV was used. Samples for TEM were collected by dipping Formvar-coated, carbon-reinforced copper electron grids by slow dipping through the air–water interface. Excess fluid, collected during the dipping process, was removed immediately with filter paper, and the grids were left to dry in air. Immature crystals were examined during the early stages of development ($t = 10\text{--}30$ min after spreading of the surfactant) using a JEOL 2000FX high-resolution analytical electron microscope operating at 200 kV. Selected area electron diffraction patterns were recorded from the crystals. Crystallographic indices are presented in the three-index notation, using $[uvw]$ axes and (hkl) faces, and are based on the unit cell of calcite.

Results and Discussion

Characterization of the Template. Aqueous dispersions (0.1%, w/v) of phospholipid **1** were prepared by injecting an aqueous solution (2% (w/v)) of these compounds in water followed by sonicating at 60 °C for 15 min and subsequent aging overnight. Inspection of the samples with transmission electron microscopy revealed the formation of ribbons (Figure 1a). Addition of calcium ions to aqueous dispersions of **1** caused the formation of tubular structures (Figure 1b) with diameters ranging from 20 to 40 nm. The finding that addition of calcium ions further

(22) Kitano, Y. *Bull. Chem. Soc. Jpn.* **1962**, *32*, 1980. For further experimental details, see: (b) Rajam, S.; Heywood, B. R.; Walker, J. B. A.; Mann, S.; Davey, R. J.; Birchall, J. D. *J. Chem. Soc., Faraday Trans.* **1991**, *87*, 727. (c) Heywood, B. R.; Rajam, S.; Mann, S. *J. Chem. Soc., Faraday Trans.* **1991**, *87*, 735.

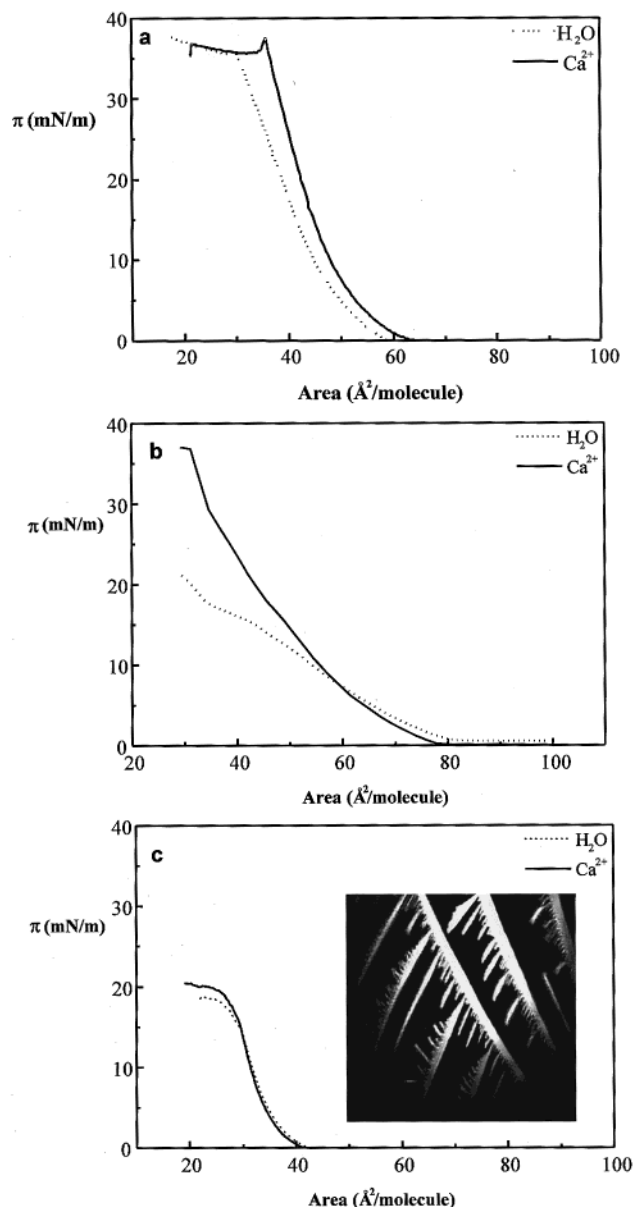


Figure 2. π - A isotherms of monolayers of (a) **1**, (b) **2**, and (c) **3** at 20 °C on (—) H_2O and (---) aqueous 10 mM CaCl_2 . Inset to part c: Brewster angle micrograph of a surface monolayer of **3** on water at 20 °C and $\pi = 0$ mN/m.

enhances the organization of these phospholipid molecules in the aggregates suggested that Langmuir films of these molecules could indeed be interesting templates for the crystallization of CaCO_3 .

For a Langmuir monolayer of compound **1** surface pressure-surface area (π - A) isotherms were recorded from which a molecular area of 50 \AA^2 was estimated by extrapolation of the curve to zero pressure. When spread on a subphase containing 9 mM CaCl_2 , compound **1** exhibited a significant interaction with the calcium ions present, as was deduced from a faster build-up of the surface pressure upon compression (Figure 2a). However, calcium complexation did not induce changes in the extrapolated molecular area. The observed higher lift-off area in the presence of Ca^{2+} suggests an increase in steric interactions between the molecules upon compression of the monolayer, which is attributed to interlinking of neighboring "amide polymer chains"¹⁷ through complexation of calcium ions. The film collapses at a limiting molecular area of 36 \AA^2 when calcium ions are present

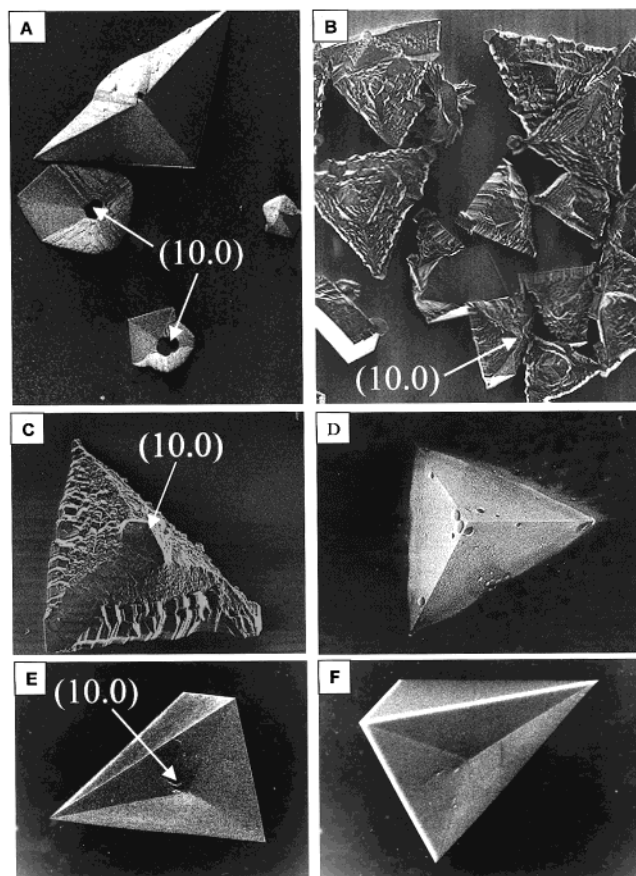


Figure 3. Scanning electron micrographs of calcite crystals grown (a) under liquidlike ($60 \text{ \AA}^2/\text{molecule}$, $\pi \sim 3$ mN/m) and (b-d) in solidlike ($40 \text{ \AA}^2/\text{molecule}$, $\pi \sim 25$ mN/m) monolayers of **1** and (e and f) under a solidlike ($40 \text{ \AA}^2/\text{molecule}$, $\pi \sim 25$ mN/m) monolayer of **2**. Bars represent $10 \mu\text{m}$.

and at 30 \AA^2 when Ca^{2+} is absent, indicating that Ca^{2+} ions position themselves between the lipid headgroups.

Crystallization Experiments. Crystallization of calcium carbonate beneath a monolayer of **1** in its liquid state ($A = 60 \text{ \AA}^2$, $\pi = 3$ mN/m) resulted in the formation of oriented and discrete calcite crystals. Viewed from above the monolayer surface, the crystals had prismatic shapes with two $\{10.4\}$ faces being expressed with opposite to these faces a roughened side, as was observed with scanning electron microscopy (Figure 3a).²³ In most cases a flat apex was observed indicative of the location where the monolayer acted as a nucleation site. When a monolayer of **1** in a more solidlike state was used ($A = 40 \text{ \AA}^2$; $\pi = 25$ mN/m), the nucleation density was increased viz. from 330 to 490 mm^{-2} .²⁴ In both cases these values are high compared to values ($>106 \text{ mm}^{-2}$) reported for the nucleation of CaCO_3 under monolayers at the air-water interface;¹¹ much higher values were obtained for self-

(23) In studies on templating monolayers, the formation of two types of calcite is observed; see ref 22b and: Mann, S.; Heywood, B. R.; Rajam, S.; Walker, J. B. A. *ACS Symp. Ser.* **1991**, *444*, 28. Type I exhibits pseudo- C_2 symmetry with all four basal $\{10.4\}$ faces expressed. Type II has pseudo- C_s symmetry and is triangular in projection with only two of the four basal edges being expressed. Type II calcite can be formed through nucleation from different faces, that is, $[00.1]$ (*n*-eicosyl sulphate) and $[1-10]$ (stearic acid). The calcite formed in the present case is of type II and has nucleated from the $\{10.0\}$ face. Type I calcite is thought to arise from a realignment and subsequent secondary growth of type II calcite at the monolayer surface.

(24) Under liquid expanded monolayers also a small amount of type I vaterite was formed (approximately 15% of the crystals). When the experiments were performed under compressed monolayers, this number was reduced to approximately 8%.

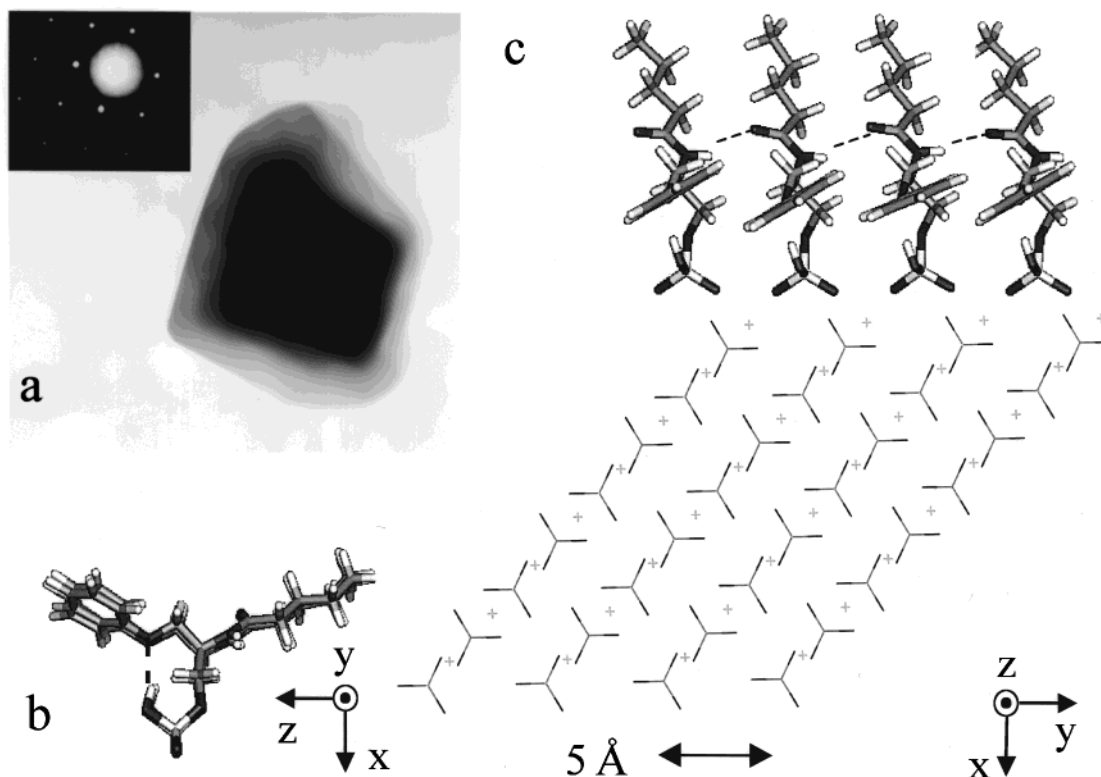


Figure 4. (a) Transmission electron micrograph and selected area electron diffraction pattern of an early [10.0] oriented calcite crystal grown under a monolayer of **1**. (b–c) Computer generated models (b) of an assembly of molecules of **1** (viewed along the y -axis) showing the hydrogen bond between the phosphate group and the ether oxygen (the number of methylene groups in the alkyl chains is reduced for reasons of clarity) and (c) of the epitaxial matching of the (10.0) face of calcite (generated with Cerius,² “+” signs represent Ca^{2+} ions) with the phosphate oxygens in an assembly of molecules of **1**. The Cartesian axes (x , y , z) match the crystallographic axes (a , b , c).

assembled monolayers on gold.⁹ The morphological form of these crystals still was prismatic; however, in this case stepped surfaces were observed (Figure 3b). These stepped faces suggest a significant interaction of the growing crystal with the lipid monolayer. In contrast, when viewed from below the monolayer, smooth {10.4} rhombohedral faces were observed, indicating that with time the crystals grow free of the constriction of the monolayer and down into the calcium carbonate solution (Figure 3d). Electron diffraction studies were performed on crystals removed from the two crystallization assays after 10–30 min (Figure 4a). The observed patterns confirmed the formation of the calcite nature of the crystals and showed that the (10.0) face had been nucleated by the monolayer in both cases. This is remarkable, since monolayers both of phosphates^{16b} and of phosphonates have been shown to nucleate the (00.1) face of calcite. In these cases the orientation of the carbonate ions was found to match the lattice of the template in which the phosphate and phosphonate headgroups possess a “tridentate” orientation, that is, an orientation in which three of the phosphate oxygen atoms are in the plane of the nucleated crystal face.

It was demonstrated in previous work that the amide hydrogen bonds fix the molecules of **1** in a linear array with an intermolecular distance of approximately 5 Å.¹⁷ Furthermore, it was indicated by FT-IR studies in conjunction with molecular modeling that an intramolecular hydrogen bond between one of the P–O–H groups and its ether oxygen was formed when the charges on the phosphate headgroups were compensated by protonation.²⁵ In this situation the molecules of **1** adopt an arrangement in which the phosphate groups bend back, leaving only two of the phosphate oxygen atoms in contact

with the aqueous phase, parallel to the “amide polymers” (Figure 4b). We propose that the charge compensation arising from calcium ion binding leads to a similar bidentate headgroup structure with a 5 Å repeat distance (Figure 4c). This motif indeed matches the orientation and spacing (4.99 Å) of the carbonate ions along the b -axis in the (10.0) crystal face of calcite. In contrast, the molecular area of 50 Å² suggests that the interarray distance is 10 Å, which does not correspond very well to the carbonate–carbonate repeat distance of 8.53 Å in this plane. However, the π - A isotherm shows that the molecules **1** can be compressed to an area of 36 Å²/molecule before the film ruptures, implying that a more dense packing which better matches the lattice spacings is well possible. Moreover, it has been demonstrated that the stereochemical and electrostatic matching can override quite well the necessity of exact epitaxial matching of the lattice dimensions.^{11a,16a}

Effect of Headgroup Orientation on Epitaxial Matching. To verify the proposed templating mechanism, that is, the necessity of hydrogen bond formation and bidentate orientation of the headgroup for the epitaxial matching of the (10.0) crystal plane, compound **2** was prepared which carried one methyl substituent on its phosphate group. Under the conditions applied, the methylated phosphate moiety of **2** cannot form a hydrogen bond with the phenoxy group, and therefore, its headgroup will be conformationally less restricted than the phosphate group of **1**. The interaction of **2** with calcium ions was again investigated first in aqueous dispersion, leading to the formation of left-handed helically wound multilayered

(25) Lowering the pH also resulted in a higher degree of headgroup organization and in the formation of helical ribbons.¹⁷

ribbons (Figure 1c) with widths of 300–400 nm and a pitch of 1.0 μm .

The π - A isotherms obtained from this compound (Figure 2b) showed that the higher conformational freedom and the larger steric repulsion of the methylated phosphate groups lead to the formation of a less preorganized monolayer. The complexation of calcium ions led to an increase in the organization of **2**, but the observed lift-off area and compressibility indicate that the molecules still have a lower tendency to pack in a compressed monolayer than those of **1**. The compression isotherm revealed a molecular area of 48 $\text{\AA}^2/\text{molecule}$ (deduced by extrapolation of the high-pressure part of the curve), which is close to the value obtained for compound **1**. Molecular models again suggested an intermolecular distance of 5 \AA and showed that upon application of lateral pressure a headgroup structure similar to that of **1**, that is, a bidentate motif of the phosphate groups, is possible (Figure 4b). From this it was expected that only compressed monolayers of **2** could match the (10.0) face of calcite.

Indeed, CaCO_3 grown under monolayers of **2** in the liquid expanded state gave almost no oriented crystals but randomly intergrown rhombohedral calcite (not shown). However, when monolayers in the compressed state were used as templates ($A = 40 \text{\AA}^2$, $\pi = 23 \text{ mN/m}$), oriented calcite crystals were observed (Figure 3e and f). These crystals had distorted trigonal bipyramidal shapes with a small apex on of the top. The presumption that in a compressed monolayer the arrangement of the phosphate headgroups of **2** matches the (10.0) face of calcite was confirmed by electron diffraction performed on crystals recovered from the assay after 10–30 min. The nucleation density of oriented crystal growth using films consisting of molecules of **2** was found to be significantly lower than that of **1** (approximately 50 mm^{-2}), reflecting the lower degree of molecular organization in the template.²⁶

To unequivocally establish the specificity of the templating effect, that is, to prove that the action of the phosphate group is essential and that the selective nucleation of the (10.0) face is not due to the presence of the other parts of the molecules, compound **3** was used as a control. Surface pressure–surface area (π - A) isotherms were recorded from which it was calculated that on a water subphase compound **3** had a molecular area of 38 $\text{\AA}^2/\text{molecule}$.²⁷ This compound was found to generate a

condensed film upon compression (Figure 2c). Brewster angle microscopy²⁸ (BAM) revealed that already at zero pressure very large 2D crystalline domains with dimensions on the order of millimeters were present. (Figure 2c, inset).²⁹ When **3** was spread on an aqueous 9 mM CaCl_2 subphase, both the isotherm and BAM images were identical to those obtained on pure water, suggesting that the calcium ions did not interact with the monolayer. Crystallization experiments under monolayers of **3** did not reveal any interactions between the organic and the inorganic phases. After 20 h the predominant polymorph was calcite in the form of randomly intergrown rhombohedral crystals (not shown) which displayed no evidence of any preferred crystallographic orientation.

Conclusion

We have demonstrated that, in the presence of calcium ions, amide-containing phospholipid **1** self-assembles to form well-defined two-dimensional domains that subsequently serve as templates for the crystallization of calcium carbonate. This leads to the efficient nucleation and growth of [10.0] oriented calcite irrespective of the surface concentration of the lipid. Responsible for this unexpected preference for nucleation at the (10.0) face is the high degree of organization in the self-assembled monolayers, in conjunction with the restricted conformational freedom of the headgroup of the molecule. This limited mobility is due to the formation of an intramolecular hydrogen bond between the phosphate group and the phenoxy moiety which forces the phosphate group to adopt a bidentate orientation toward the aqueous phase. It was shown that when this hydrogen bond was absent, lateral pressure was required in order to enforce a similar conformation and accomplish the nucleation of [10.0] oriented calcite.

Acknowledgment. The authors would like to thank A.E. Rowan (University of Nijmegen) for the molecular modeling and S.J. Williams (Keele University) for helpful discussions.

LA001765N

(28) Hönig, D.; Möbius, D. *J. Chem. Phys.* **1991**, *95*, 4590. (b) Hénon, C. A.; Meunier, J. *Rev. Sci. Instrum.* **1991**, *62*, 936.

(29) The high degree of organization of the molecules of **3**, as apparent from the Brewster angle micrographs, suggests the presence of a strong hydrogen bonding network. CPK models indeed indicate that, in addition to the expected formation of linear arrays of amide groups,¹⁷ hydrogen bonds could be formed between the hydroxyl functions and the oxygen atoms of the phenoxy groups in neighboring molecules. The molecular area of 40 \AA^2 deduced from these models is in good agreement with the value obtained from the π - A isotherm.

(26) In addition, a significant amount of vaterite crystals was observed.

(27) Surfactant **3** was insoluble in water, and no distinct aggregate morphology could therefore be detected by transmission electron microscopy.